

1

2 Supporting Information for:

3 Reactivity of the Polyamide Membrane Monomer with

4 Free Chlorine: Reaction Kinetics, Mechanisms, and the

5 Role of Chloride

6 *Kun Huang[†], Keith P. Reber[§], Michael D. Toomey[‡], Holly Haflich^{||}, John A. Howarter^{‡,||}, and*

7 *Amisha D. Shah^{*,†,||}*

8

9 [†] Lyles School of Civil Engineering, Purdue University, 550 Stadium Mall Drive, West

10 Lafayette, Indiana 47907, United States

11 [§] Department of Chemistry, Towson University, 8000 York Road, Towson, Maryland

12 21252, United States

13 [‡] School of Materials Engineering, Purdue University, 701 W. Stadium Avenue, West Lafayette,

14 Indiana 47907, United States

15 ^{||} Division of Environmental and Ecological Engineering, Purdue University, 500 Central Drive,

16 West Lafayette, Indiana 47907, United States

17

18 * Corresponding author phone: 765-496-2470; fax: 765-494-0395; e-mail: adshah@purdue.edu

19

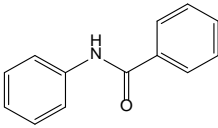
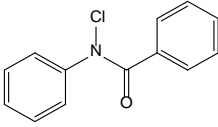
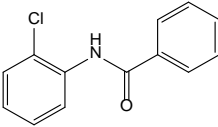
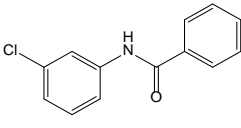
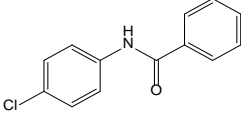
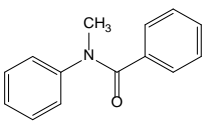
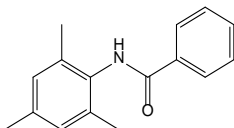
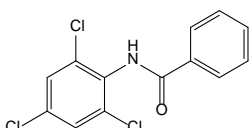
20 33 Pages

21 5 Tables

22 16 Figures

23 8 Text Sections

24 **Table S1.** Compound names, structures and acronyms used in this study.

Compound Names	Structures	Acronyms
benzanilide		BA
<i>Expected BA By-products:</i>		
<i>N</i> -chloro- <i>N</i> -phenylbenzamide		<i>N</i> -Cl-BA
<i>N</i> -(2-chlorophenyl)benzamide		<i>o</i> -Cl-BA
<i>N</i> -(3-chlorophenyl)benzamide		<i>m</i> -Cl-BA
<i>N</i> -(4-chlorophenyl)benzamide		<i>p</i> -Cl-BA
<i>Structurally Modified Compounds</i>		
<i>N</i> -methyl- <i>N</i> -phenylbenzamide		<i>N</i> -CH ₃ -BA
<i>N</i> -mesitylbenzamide		2,4,6-(CH ₃) ₃ -BA
<i>N</i> -(2,4,6-trichlorophenyl)benzamide		2,4,6-Cl ₃ -BA

25

26

27 **Table S2.** Summary of the reaction conditions used for each kinetic experiment.

Type	pH	Model compound	Model compound concentration (μM)	Free chlorine (mM) ^a	Cl ⁻ (mM)		
					Amended	From the background ^b	Total
1	4.0-9.0	BA	8.1-11	0.2-0.5	0	0.23-0.58	0.23-0.58
	7.0	<i>N</i> -CH ₃ -BA	11	0.2	0	0.27	0.27
	7.0	2,4,6-(CH ₃) ₃ -BA	8.3	0.2	0	0.27	0.27
	7.0	2,4,6-Cl ₃ -BA	10	0.2	0	0.27	0.27
2	4.0-7.0	BA	7.9-11	0.2	60-540	0.23-0.27	60-540
	3.9	<i>N</i> -CH ₃ -BA	11	0.2	540	0.23	540
3 ^c	4.0	<i>N</i> -Cl-BA	30 ^d	0	540	0	540

28 ^a These values are the targeted initial concentrations. The actual concentrations of free chlorine ranged from 0.19-0.23 mM.

29 ^b The values included Cl⁻ concentrations from the free chlorine stock and buffer solutions.

30 ^c This experiment was conducted to specifically evaluate the Orton rearrangement.

31 ^d The concentration of *N*-Cl-BA was determined by using an approximate purity of 80%, which was measured by GC/MS in the same week that this experiment
 32 was run. The initial total mass of the *N*-Cl mix added to the reaction solution was 8.8 mg/L.

Table S3. Species-specific rate constants for the *N*-chlorination of secondary amides (R₁-C(O)NH-R₂)

R₁	R₂	k_{HOCl} (M⁻¹s⁻¹)¹	k_{OCl-} (M⁻¹s⁻¹)¹
CH ₃	CH ₃	1.7×10 ⁻³	1.82×10 ⁻²
H	CH ₂ CH ₃	1.7×10 ⁻³	1.15×10 ⁻¹
H	CH ₃	1.7×10 ⁻³	2.1×10 ⁻¹

Table S4. Details regarding the physical properties, column retention, and ions extracted for the compounds analyzed by GC/MS.

Analyte	MW (g/mole)	Retention Time (min)	Ions Used for Quantitative or Qualitative Analysis
naphthalene-d8	136.2	5.36	136^a
BA	197.2	9.20	105 , 197
<i>N</i> -Cl-BA ^b	231.7	8.93	105 , 197
<i>o</i> -Cl-BA	231.7	9.46	105, 196 , 231
<i>p</i> -Cl-BA	231.7	10.28	105 , 231
<i>m</i> -Cl-BA	231.7	10.31	105 , 231
2,4,6-Cl ₃ -BA	300.6	11.38	105 , 264, 266
2,4,6-(CH ₃) ₃ -BA	239.3	10.16	239

^a bold values represented the base peaks

^b only a qualitative assessment was made for this compound

Table S5. Equilibrium concentrations of chlorinating agents under different conditions.

pH	[HOCl] ₀ (μM)	[Cl ⁻] ₀ (mM)	[HOCl] _{eq} (M)	[Cl ₂] _{eq} (M)	[Cl ₂ O] _{eq} (M)	[OCl ⁻] _{eq} (M)
4.0	200	0.23	2.0×10 ⁻⁴	1.2×10 ⁻⁸	3.5×10 ⁻¹⁰	5.5×10 ⁻⁸
6.2	200	0.27	1.9×10 ⁻⁴	8.2×10 ⁻¹¹	3.2×10 ⁻¹⁰	8.8×10 ⁻⁶
6.5	200	0.27	1.8×10 ⁻⁴	3.7×10 ⁻¹¹	2.9×10 ⁻¹⁰	1.8×10 ⁻⁵
7.0	200	0.27	1.5×10 ⁻⁴	1.0×10 ⁻¹¹	2.1×10 ⁻¹⁰	4.7×10 ⁻⁵
9.3	200	0.24	3.6×10 ⁻⁶	1.2×10 ⁻¹⁵	1.1×10 ⁻¹³	2.0×10 ⁻⁴
7.0	200	60	1.7×10 ⁻⁴	3.7×10 ⁻⁹	2.4×10 ⁻¹⁰	3.3×10 ⁻⁵
6.5	200	540	1.9×10 ⁻⁴	9.9×10 ⁻⁸	3.0×10 ⁻¹⁰	1.4×10 ⁻⁵
4.1	350	0.40	3.5×10 ⁻⁴	2.6×10 ⁻⁸	1.1×10 ⁻⁹	1.4×10 ⁻⁷
4.2	500	0.58	5.0×10 ⁻⁴	4.9×10 ⁻⁸	2.2×10 ⁻⁹	2.1×10 ⁻⁷
4.1	200	20	2.0×10 ⁻⁴	7.8×10 ⁻⁷	3.5×10 ⁻¹⁰	7.4×10 ⁻⁸
4.1	200	50	2.0×10 ⁻⁴	2.2×10 ⁻⁶	3.4×10 ⁻¹⁰	6.3×10 ⁻⁸
4.1	200	80	2.0×10 ⁻⁴	3.9×10 ⁻⁶	3.4×10 ⁻¹⁰	5.8×10 ⁻⁸
4.0	200	540	1.7×10 ⁻⁴	3.1×10 ⁻⁵	2.5×10 ⁻¹⁰	3.6×10 ⁻⁸

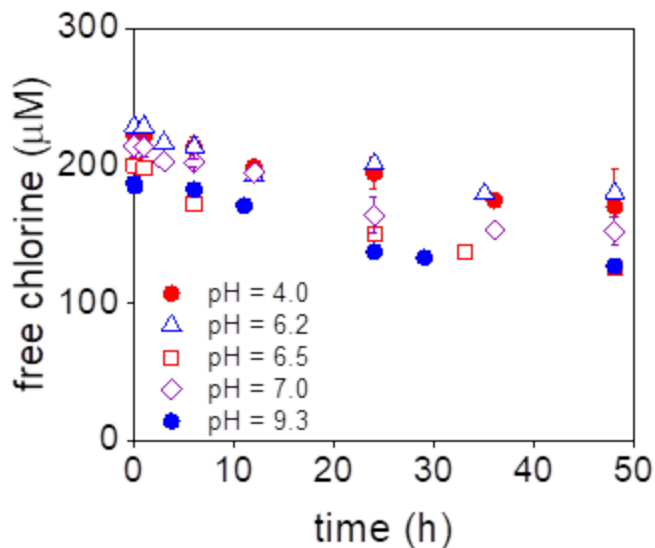


Figure S1. Loss of free chlorine versus time during its reaction of BA at pH 4.0-9.3. ($[BA]_0 = 10 \mu\text{M}$; $[\text{free chlorine}]_0 = 200 \mu\text{M}$; 10 mM acetate (pH 4.0), phosphate (pH 6.0-7.0) or borate (pH 9.2) buffer). Error bars represent the standard deviation of ≥ 3 replicates.

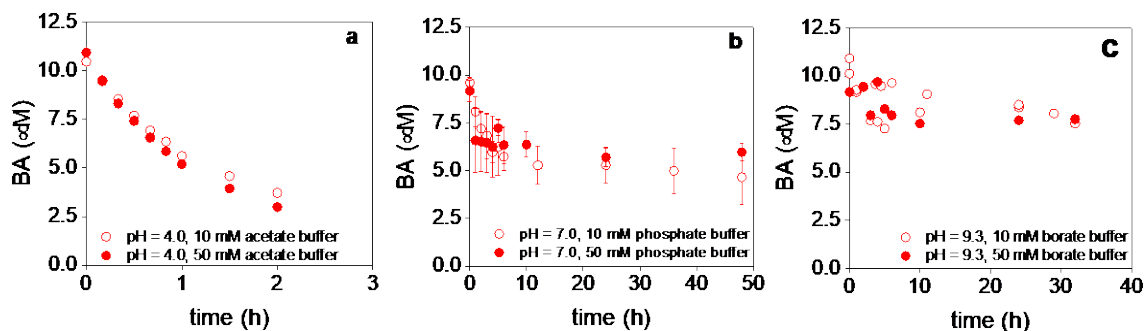


Figure S2. The effect of buffer concentrations on degradation kinetics of BA when exposed to (a) free chlorine and chloride at pH 4.0 ($[BA]_0 = 10 \mu\text{M}$; $[\text{free chlorine}]_0 = 200 \mu\text{M}$; $[\text{Cl}^-] = 80 \text{ mM}$; 10 and 50 mM acetate buffer; conducted with LC analysis with $\sim 13\%$ *N*-Cl-BA formation), (b) free chlorine alone at pH 7.0 ($[BA]_0 = 10 \mu\text{M}$; $[\text{free chlorine}]_0 = 200 \mu\text{M}$; 10 and 50 mM phosphate buffer), and (c) free chlorine alone at pH 9.3 ($[BA]_0 = 10 \mu\text{M}$; $[\text{free chlorine}]_0 = 200 \mu\text{M}$; 10 and 50 mM borate buffer).

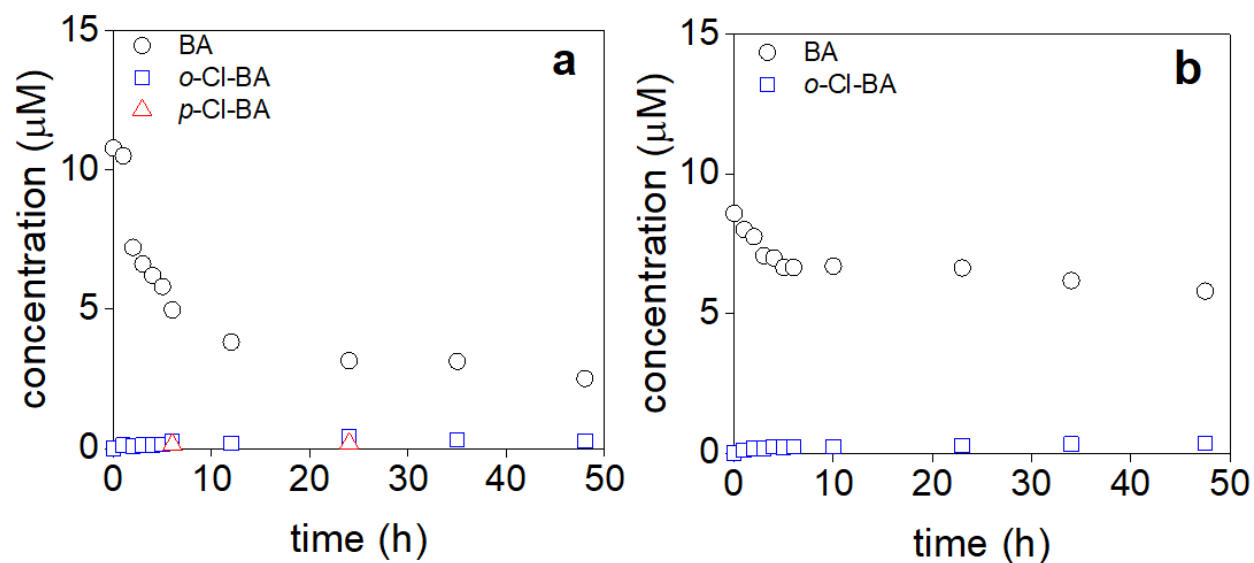


Figure S3. Product formation versus time when assessing BA reacting with free chlorine alone at (a) pH 6.2 and (b) pH 6.5. ($[BA]_0 = 10 \mu\text{M}$; $[\text{free chlorine}]_0 = 200 \mu\text{M}$; $[\text{Cl}^-]_0 = 0.27 \text{ mM}$; 10 mM phosphate buffer). *p*-Cl-BA was not formed at > d.l. values under pH 6.5 conditions.

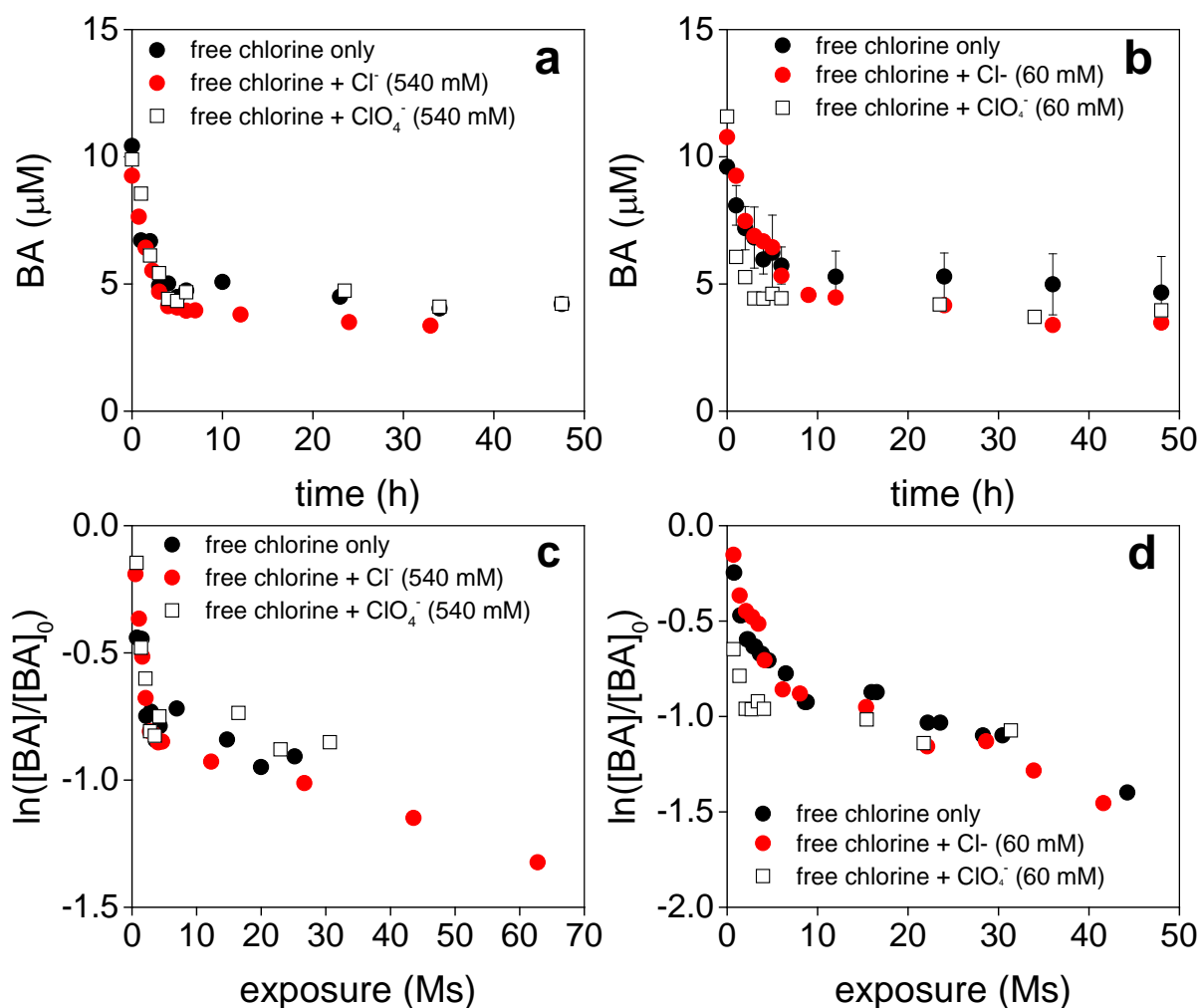


Figure S4. Loss of (a, b) BA versus time and (c, d) BA expressed as $\ln([BA]/[BA]_0)$ versus free chlorine exposure during reaction of BA with free chlorine alone, in the presence of Cl^- or ClO_4^- at (a, c) pH 6.5 and (b, d) pH 7.0. ($[BA]_0 = 10 \mu\text{M}$; $[\text{free chlorine}]_0 = 200 \mu\text{M}$; $[\text{Cl}^- \text{ or } \text{ClO}_4^-]_0 = 60 \text{ or } 540 \text{ mM}$; 10 mM phosphate buffer)

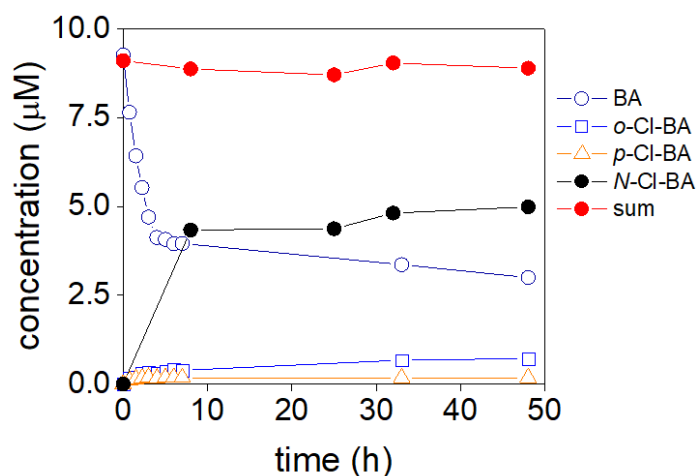


Figure S5. Product formation versus time during reaction of BA with free chlorine in the presence of Cl^- at pH 6.5. The $N\text{-Cl-BA}$ formation was indirectly quantified by SO_3^{2-} quenching approach. ($[\text{BA}]_0 = 10 \mu\text{M}$; $[\text{free chlorine}]_0 = 200 \mu\text{M}$; $[\text{Cl}^-]_0 = 540 \text{ mM}$; 10 mM phosphate buffer)

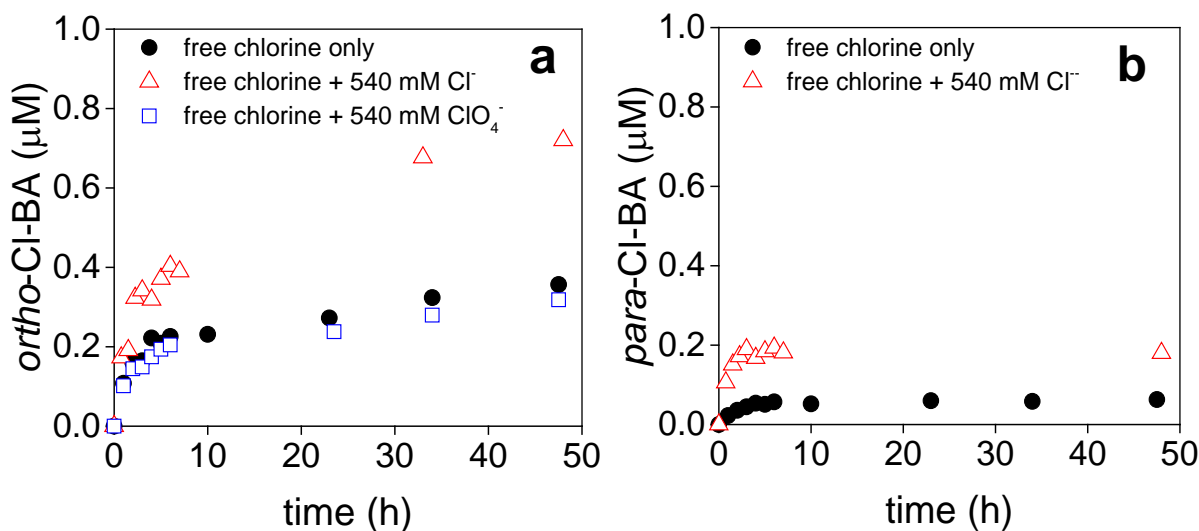


Figure S6. Formation of (a) $o\text{-Cl-BA}$ and (b) $p\text{-Cl-BA}$ during reaction of BA with free chlorine, in the presence of Cl^- or ClO_4^- . The $p\text{-Cl-BA}$ formation for free chlorine + ClO_4^- was below d.l. ($[\text{BA}]_0 = 10 \mu\text{M}$; $[\text{free chlorine}]_0 = 200 \mu\text{M}$; $[\text{Cl}^- \text{ or } \text{ClO}_4^-]_0 = 540 \text{ mM}$; pH 6.5; 10 mM phosphate buffer)

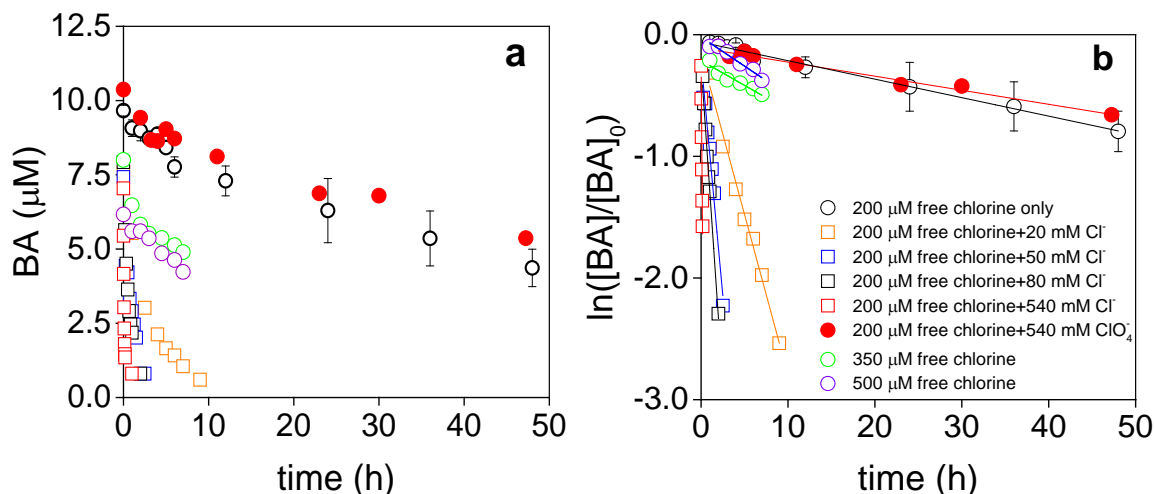


Figure S7. (a) Degradation and (b) exponential loss of BA versus time during its reaction with free chlorine alone and with or without Cl⁻ or ClO₄⁻ at pH 4.0. ([BA]₀ = 10 μM; [free chlorine]₀ = 200-500 μM; [Cl⁻ or ClO₄⁻]₀ = 0.23-540 mM; 10 mM acetate buffer)

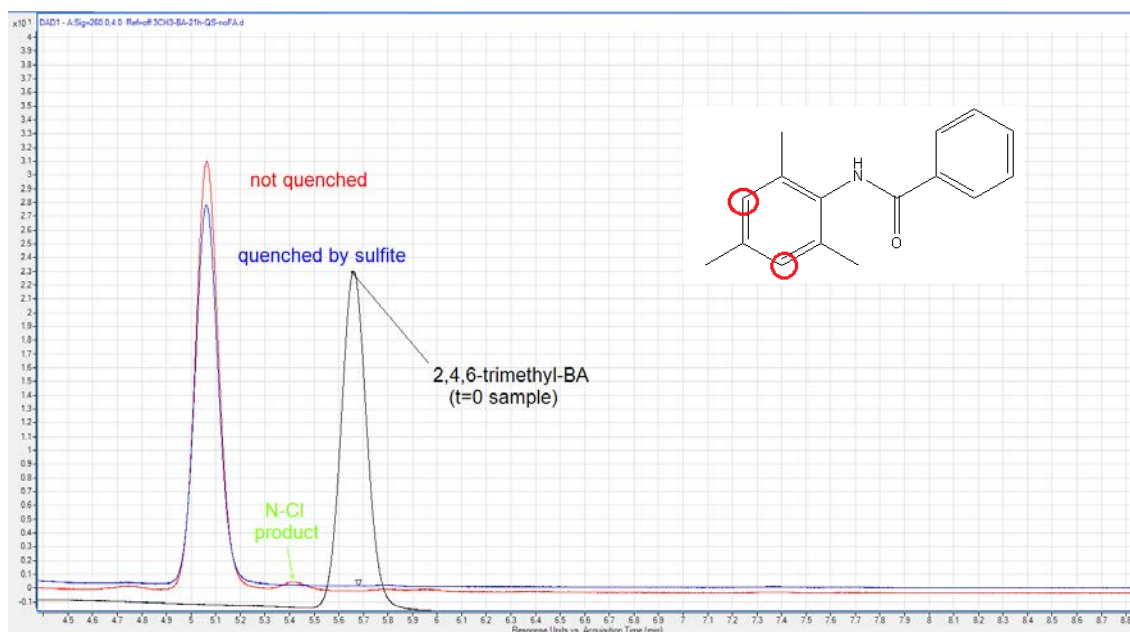


Figure S8. The overlaid chromatograms of the unreacted 2,4,6-(CH₃)₃-BA (t=0 h sample), unquenched sample and the sample quenched by sulfite during reaction of 2,4,6-(CH₃)₃-BA with excess free chlorine ([2,4,6-(CH₃)₃-BA]₀ = 10 μM, [free chlorine]₀ = 200 μM, pH = 7.0).

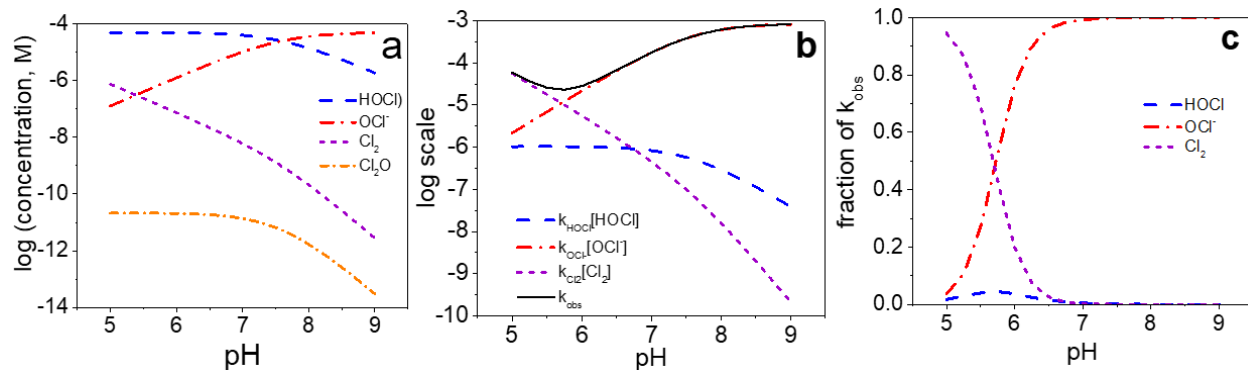


Figure S9. Model curves of (a) the chlorinating agent speciation at equilibrium, (b) the contribution of each chlorinating agent (e.g. $k_{\text{HOCl}}[\text{HOCl}]$) to the overall reaction rate (k_{obs}), and (c) fraction of each chlorinating agent to this rate (e.g. $k_{\text{HOCl}}[\text{HOCl}]/k_{\text{obs}}$). Model was run using conditions typically used for the RO treatment of seawater when chlorination is applied for biofouling control ([free chlorine] = 3.55 mg/L as Cl₂ (mean value of typical 2-5 mg/L-Cl₂ range² (50 μM), [Cl⁻] = 19 g/L (0.54 M³), ionic strength was calculated using the ionic compositions of typical seawater⁴, 25 °C)

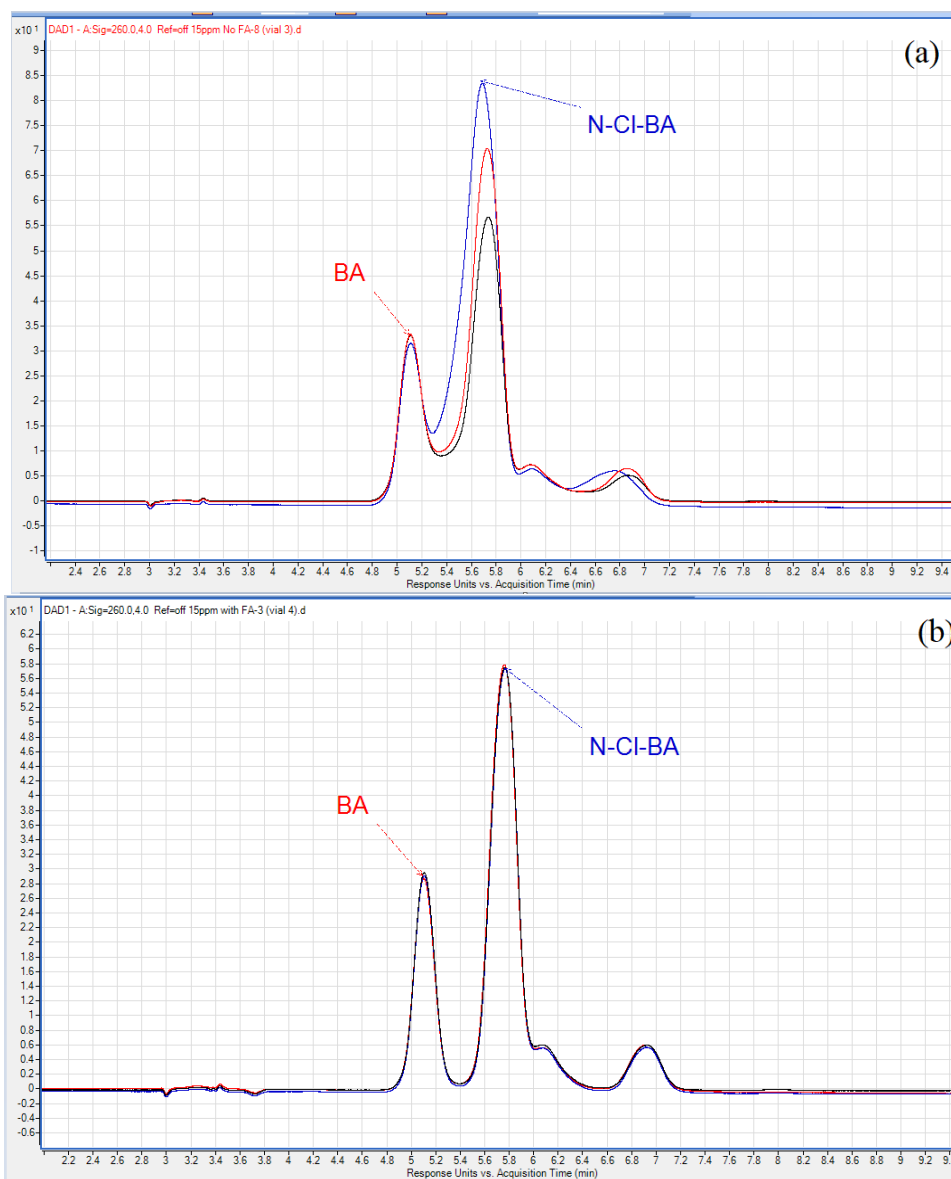


Figure S10. An overlay of three HPLC/DAD chromatograms from three different injections of the *N*-Cl mix (15 mg/L) which either (a) did not contain formic acid in the eluent or (b) did contain formic acid in the eluent.

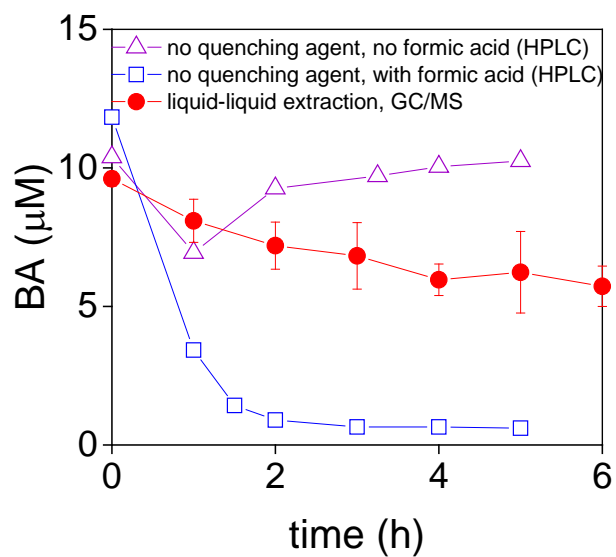


Figure S11. Comparison between the kinetic data obtained when not adding a quenching agent to the reaction, with and without formic acid in the HPLC eluent, with that obtained when quenched by liquid/liquid extraction and measured by the GC/MS. ($[BA]_0 = 9.5\text{-}12\text{ }\mu\text{M}$, $[\text{free chlorine}]_0 = 200\text{ }\mu\text{M}$, pH 7.0, 10 mM phosphate buffer).

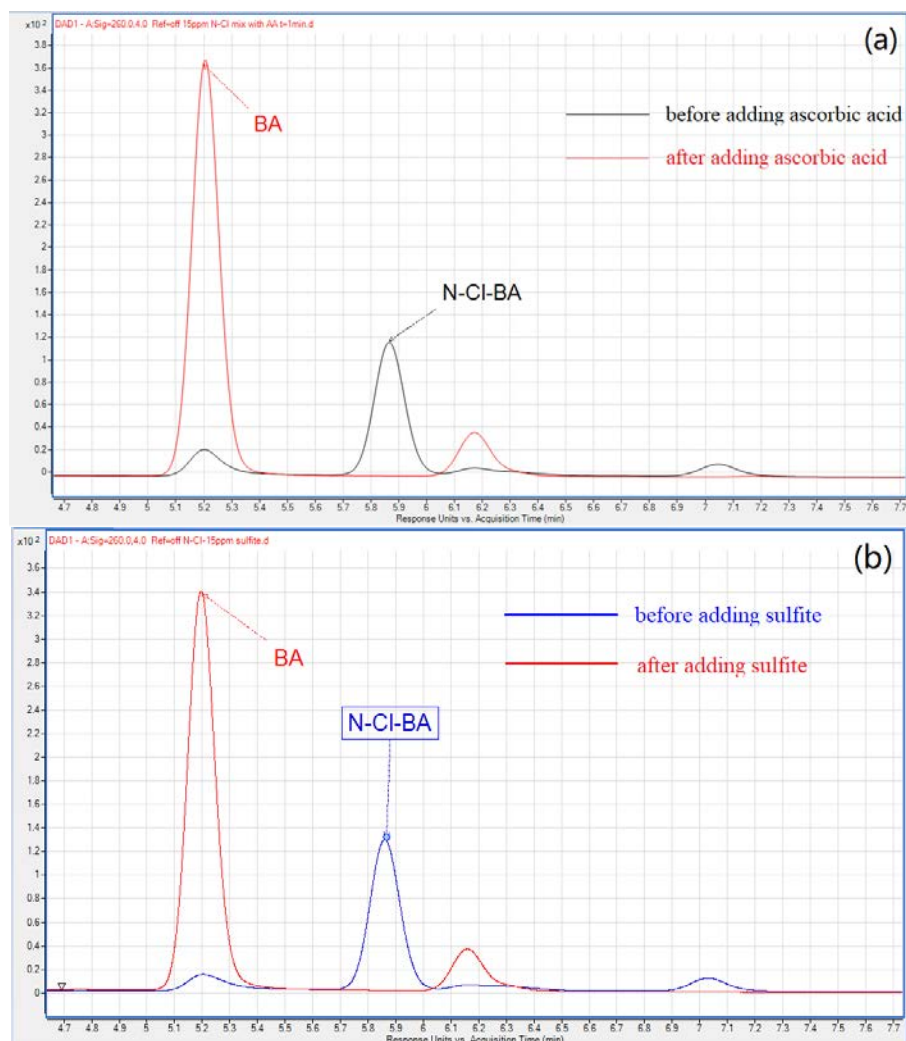


Figure S12. The overlaid chromatograms before and after the *N*-Cl mix was exposed to (a) ascorbic acid and (b) SO_3^{2-} . ($[\text{N-Cl mix}] = 15 \text{ mg/L}$; $[\text{ascorbic acid or } \text{SO}_3^{2-}]_0 = 0.4 \text{ mM}$; $[\text{ascorbic acid}]_0/[\text{N-Cl-BA}]_0 \approx 9.3$; pH 7.0 with 10 mM phosphate buffer).

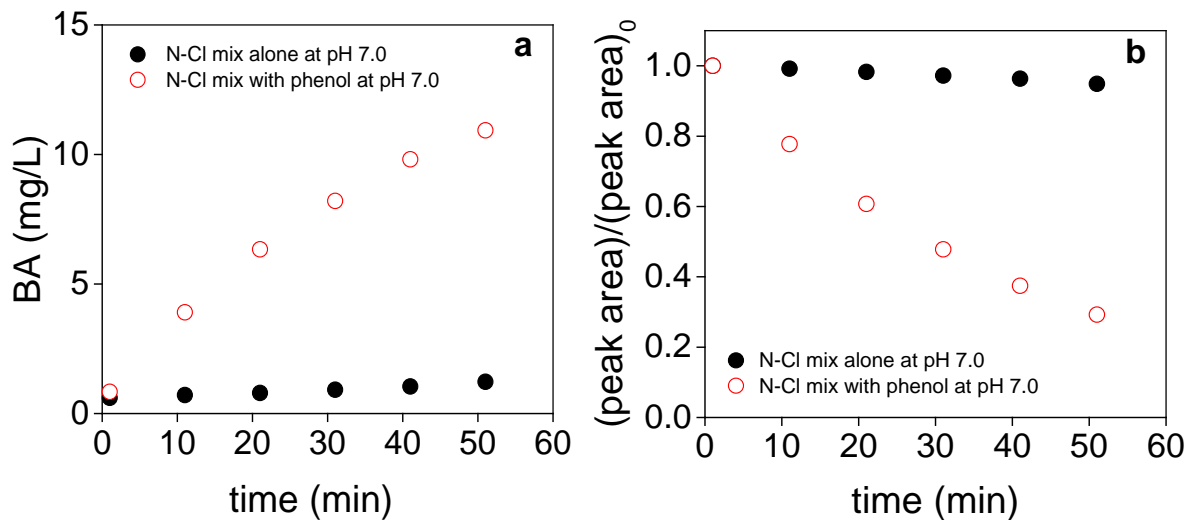


Figure S13. Effect of phenol in converting *N*-Cl-BA back into BA as noted by the changing (a) BA concentration and (b) *N*-Cl-BA peak area over time. ($[N\text{-Cl mix}]_0 = 20 \text{ mg/L}$, $[\text{phenol}]_0 = 10 \text{ mM}$, $\text{pH} = 7.0$, 10 mM phosphate buffer).

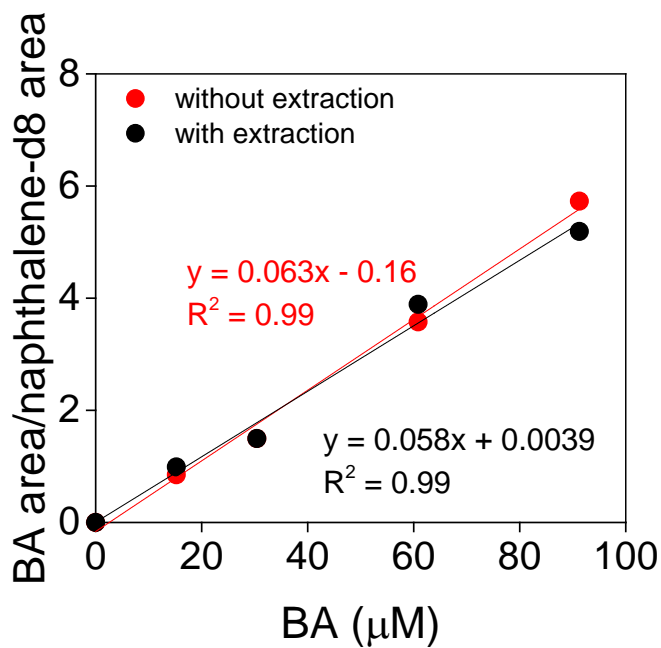


Figure S14. Comparison of the BA calibration curves obtained with and without extraction in order to assess its recovery. The y-axis represented the ratio of BA area to naphthalene-d8 (internal standard) area.

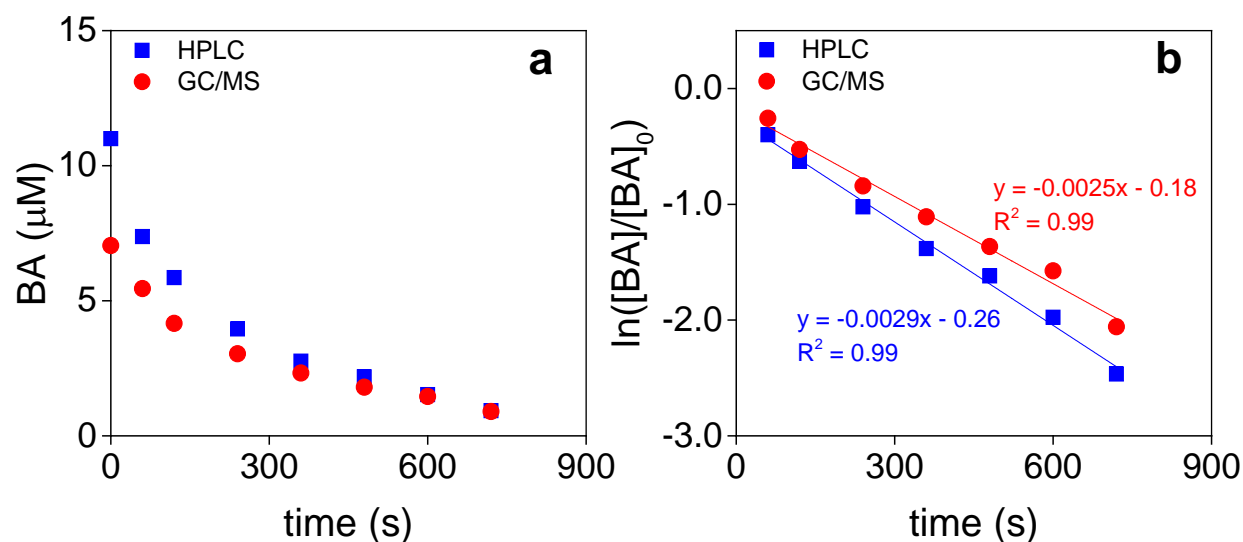


Figure S15. Comparison of SO_3^{2-} quenching coupled with HPLC (approach 1) and liquid extraction coupled with GC/MS (approach 2) for reactions of BA with free chlorine in the presence of Cl^- at pH 4.0 ($[\text{BA}]_0 = 7\text{--}11\ \mu\text{M}$, $[\text{HOCl}]_0 = 200\ \mu\text{M}$, $[\text{Cl}^-]_0 = 540\ \text{mM}$, 10 mM acetate buffer).

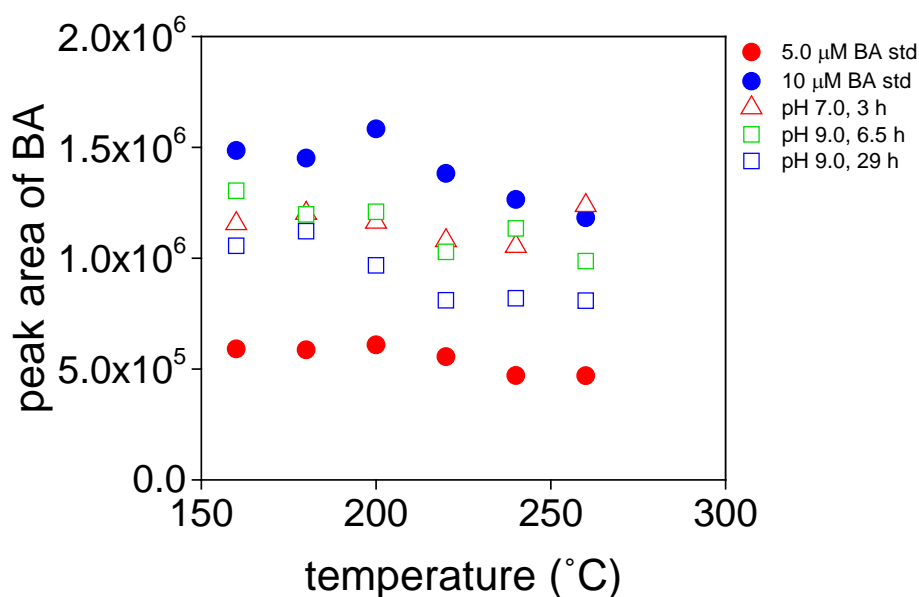


Figure S16. The BA peak areas as a function of injection port temperature when either injecting two BA standards ($[\text{BA}]_0 = 5.0$ and $10\ \mu\text{M}$) or three samples in which BA reacted with free chlorine at pH 7.0 and 9.0. ($[\text{BA}]_0 = 10\ \mu\text{M}$, $[\text{free chlorine}]_0 = 200\ \mu\text{M}$, 10 mM phosphate (7.0) or borate (9.0) buffer).

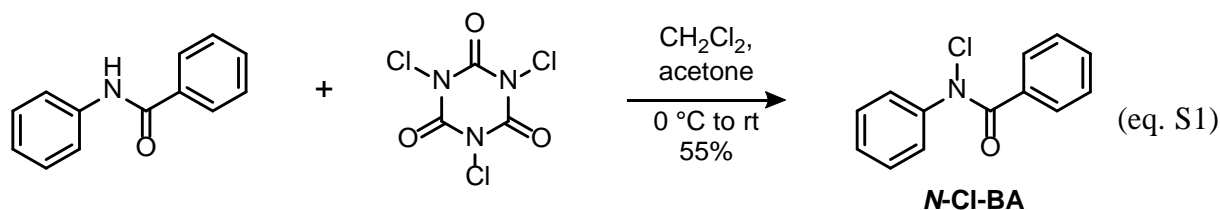
Text S1. Description of commercially purchased standards and reagents.

The standards and reagents used for these experiments included: (i) phenol, sodium hypochlorite (13% w/w), ascorbic acid, sodium sulfite, acetic acid, and sodium acetate which were purchased from Acros Organics, (ii) BA and naphthalene-d8 which were purchased from Sigma-Aldrich, (iii) 2,4,6-Cl₃-BA ($\geq 90\%$ purity) which was purchased from Mcule, Inc. (Palo Alto, CA), and (iv) 2,4,6-(CH₃)₃-BA ($\geq 90\%$ purity) which was purchased from ChemBridge Corporation (San Diego, CA). These and other chemicals, such as NaCl, Na₂HPO₄·2H₂O, NaH₂PO₄·H₂O, Na₂B₄O₇·10 H₂O, MeOH, dichloromethane (DCM) and acetonitrile (CH₃CN; ACN) were purchased at reagent grade or higher and used without further purification.

Text S2. Synthesis methods and purities of the *N*-Cl-BA, *p*-Cl-BA, *o*-Cl-BA, *m*-Cl-BA and *N*-CH₃-BA standards.

Several compounds were synthesized, including *N*-Cl-BA, *p*-Cl-BA, *m*-Cl-BA, *o*-Cl-BA, and *N*-CH₃-BA. Their synthesis methods are provided below:

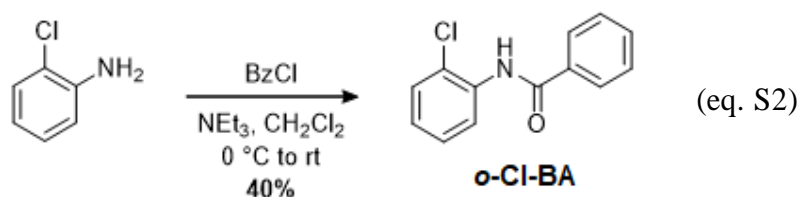
Synthesis methods for N-Cl-BA



To a 50 mL flask equipped with a magnetic stirring bar was added a solution of benzanilide (500 mg, 2.54 mmol, 1.00 eq.) in 20 mL of DCM (CH₂Cl₂) and 5 mL of acetone. This solution was cooled to 0 °C in an ice bath, and solid trichlorisocyanuric acid (TCA, 206 mg, 0.84 mmol, 0.35 eq.) was added in a single portion (eq. S1). The cooling bath was removed, and the clear,

colorless, homogeneous reaction mixture was left to stir at room temperature. After six hours, TLC (4:1 hexanes / ethyl acetate, UV / anisaldehyde stain) showed formation of the *p*-Cl-BA (R_f = 0.29, copolar with benzanilide), *N*-Cl-BA (R_f = 0.41, stains white), and a small amount of the *o*-Cl-BA (R_f = 0.48). The accumulated solids were removed by filtration through Celite, and the filtrate was evaporated under reduced pressure. The crude product mixture was dissolved in ethyl acetate and washed sequentially with water and saturated aqueous sodium chloride solution before drying over anhydrous sodium sulfate. The drying agent was removed by vacuum filtration, and the filtrate was evaporated under reduced pressure. The crude product was then purified by column chromatography on silica gel eluting with 4:1 hexanes / ethyl acetate to give the pure *N*-Cl-BA as a white solid (323 mg, molar conversion = 55%). A similar synthetic method has been reported in another study.⁵

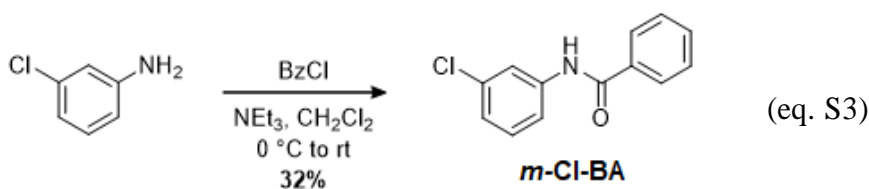
Synthesis methods for *o*-Cl-BA



To a 100 mL flask equipped with a magnetic stirring bar was added a solution of 2-chloroaniline (1.00 g, 7.84 mmol, 1.00 eq.) in 30 mL of DCM. This solution was cooled to 0 °C in an ice bath, and neat triethylamine (NEt₃, 1.64 mL, 11.8 mmol, 1.50 eq.) was added followed by the dropwise addition of neat benzoyl chloride (910 μL, 7.84 mmol, 1.00 eq.), giving a white precipitate (eq. S2). The cooling bath was removed, and the reaction mixture was stirred at room temperature for twelve hours. After this time, the reaction was quenched with 1M aqueous hydrochloric acid solution and diluted with water and dichloromethane. The layers were

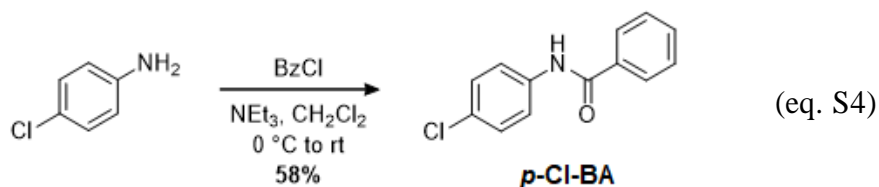
separated, and the organic phase was washed with saturated aqueous sodium bicarbonate solution before drying over anhydrous magnesium sulfate. The drying agent was removed by vacuum filtration, and the filtrate was evaporated under reduced pressure to give an off-white solid. This crude product was purified by recrystallization from 95% ethanol to give *o*-Cl-BA as a white crystalline solid (722 mg, 40%).

Synthesis methods for m-Cl-BA



To a 100 mL flask equipped with a magnetic stirring bar was added a solution of 3-chloroaniline (1.00 g, 7.84 mmol, 1.00 eq.) in 30 mL of DCM. This solution was cooled to 0 °C in an ice bath, and neat triethylamine (1.64 mL, 11.8 mmol, 1.50 eq.) was added followed by the dropwise addition of neat benzoyl chloride (910 μ L, 7.84 mmol, 1.00 eq.), giving a white precipitate (eq. S3). The cooling bath was removed, and the reaction mixture was stirred at room temperature for twelve hours. After this time, the reaction was quenched with 1M aqueous hydrochloric acid solution and diluted with water and dichloromethane. The layers were separated, and the organic phase was washed with saturated aqueous sodium bicarbonate solution before drying over anhydrous magnesium sulfate. The drying agent was removed by vacuum filtration, and the filtrate was evaporated under reduced pressure to give an off-white solid. This crude product was purified by recrystallization from 95% ethanol to give *m*-Cl-BA as a white crystalline solid (580 mg, 32%).

226 *Synthesis methods for p-Cl-BA*



227

228 To a 100 mL flask equipped with a magnetic stirring bar was added a solution of 4-

229 chloroaniline (1.00 g, 7.84 mmol, 1.00 eq.) in 30 mL of DCM. This solution was cooled to 0 °C

230 in an ice bath, and neat triethylamine (1.64 mL, 11.8 mmol, 1.50 eq.) was added followed by the

231 dropwise addition of neat benzoyl chloride (910 μ L, 7.84 mmol, 1.00 eq.), giving a white

232 precipitate (eq. S4). The cooling bath was removed, and the reaction mixture was stirred at room

233 temperature for twelve hours. After this time, the reaction was quenched with 1M aqueous

234 hydrochloric acid solution and diluted with water and DCM. The layers were separated, and the

235 organic phase was washed with saturated aqueous sodium bicarbonate solution before drying

236 over anhydrous magnesium sulfate. The drying agent was removed by vacuum filtration, and the

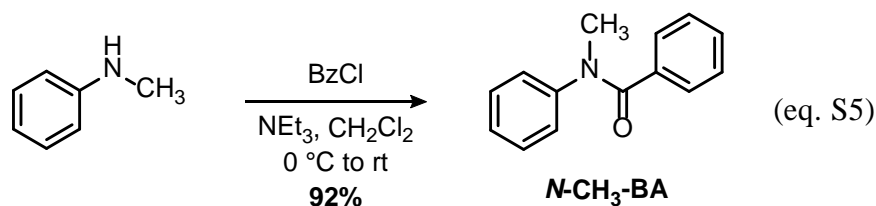
237 filtrate was evaporated under reduced pressure to give an off-white solid. This crude product was

238 purified by recrystallization from 95% ethanol to give *p*-Cl-BA as a white crystalline solid

239 (1.045 g, 58%).

240

241 *Synthesis methods for N-CH₃-BA*



242

243 To a 200 mL flask equipped with a magnetic stirring bar was added a solution of freshly

244 distilled *N*-methylaniline (1.50 g, 14.0 mmol, 1.00 eq.) in 50 mL of DCM. This solution was

cooled to 0 °C in an ice bath, and neat triethylamine (2.93 mL, 20.1 mmol, 1.50 eq.) was added followed by the dropwise addition of neat benzoyl chloride (1.62 mL, 14.0 mmol, 1.00 eq.), giving a white precipitate (eq. S5). The cooling bath was removed, and the reaction mixture was stirred at room temperature for twelve hours. After this time, the reaction was quenched with 1M aqueous hydrochloric acid solution and diluted with water and dichloromethane. The layers were separated, and the organic phase was washed with saturated aqueous sodium bicarbonate solution before drying over anhydrous magnesium sulfate. The drying agent was removed by vacuum filtration, and the filtrate was evaporated under reduced pressure to give a colorless oil. This crude product was purified by column chromatography on silica gel eluting with 3:1 hexanes / ethyl acetate ($R_f = 0.28$) to give *N*-CH₃-BA as a colorless oil (2.72 g, 92%).

Text S3. Purity of the *N*-Cl-BA standard

The *N*-Cl-BA standard was found to be unstable over 9 months when stored as a solid at either -20 or -80 °C. This instability was determined by initially measuring its purity within two weeks of arrival which was determined to be 74 and 80% when analyzed by HPLC and GC/MS, respectively. These values were measured by first noting that the other compounds present in this standard were known, including BA, *o*-, *m*-, and *p*-Cl-BA. Since standards existed for each of these compounds, their concentrations could be quantified, and the purity of the *N*-Cl-BA standard could then be calculated. After this initial assessment, the *N*-Cl-BA standard was found to change color over time, which indicated that it decomposed in some way. Its purity was never determined after this degradation occurred.

Text S4. Preparation of stock solutions.

Stock solutions of all model compounds were prepared at 3.6-25 mM in ACN, stored at -18 °C and used within one month. Free chlorine stock solutions were prepared daily in reagent water and measured spectrophotometrically by quantifying the hypochlorite (OCl^-) concentration at 292 nm ($\epsilon = 362 \text{ M}^{-1}\text{cm}^{-1}$)⁶. However, the free chlorine stock solution also contained a significant Cl^- concentration ($[\text{Cl}^-]/[\text{free chlorine}] = 1.2\text{-}1.4:1$), which was measured by ion chromatography (IC), as done previously.⁷

Text S5. Details regarding both analytical approaches.

Details regarding the two analytical approaches used in this study are as follows:

Approach 1: Sample Quenching Coupled with LC-UV/vis or LC/MS analysis. In this approach, samples were analyzed by either the HPLC with UV/vis diode-array detection (DAD) (Agilent 1260 Infinity) or by the LC/MS (Agilent 6420 Triple Quadrupole MS). Separation was achieved using an Eclipse Plus C18 column (2.5 mm \times 150 mm, 3.5 μm) in which the eluent flow rate was held at 0.3 mL/min. For the HPLC/DAD method, the mobile phase consisted of water (eluent A) and ACN with 0.1% formic acid (eluent B) in isocratic mode at 25% A/75% B for 11 min. For the LC/MS method, the mobile phase consisted of water (eluent A) and MeOH with 0.1% formic acid (eluent B) in isocratic mode for 11 min. The MS was run using electrospray ionization (ESI) in positive ion mode. The single quad was run in scan mode (m/z 50 – 400) in which the parent masses ($M+1$) of m/z 198 and 232 were quantified for BA and its chlorinated by-products (*p*-, *m*- and *o*-Cl-BA), respectively. Their identities were confirmed by cross-comparing their peaks with known standards as well as by confirming their compound molecular weights by LC/MS. This method was also used to identify and/or quantify several

model compounds including *N*-CH₃-BA, 2,4,6-(CH₃)₃-BA and 2,4,6-Cl₃-BA. The HPLC-DAD method detection limits (MDLs) for BA, *o*-Cl-BA, *p*-Cl-BA, *m*-Cl-BA, and *N*-CH₃-BA were 22, 42, 40, 15 and 51 nM, respectively. Along with these techniques, the formation of *N*-Cl-BA was also identified and indirectly quantified by adding SO₃²⁻, a strong nucleophile, which was determined to fully convert *N*-Cl-BA back to BA (see later discussions for further details). Thus, the amount of *N*-Cl-BA formed could be obtained by calculating the increase in the BA concentration after SO₃²⁻ quenching.

It should be noted that for both of the LC-based analyses, eluent B contained formic acid in order to lower the pH to 2.7. The lowered pH was important since it appeared to stabilize the chromatographic signal of the *N*-Cl-BA peak when the *N*-Cl mix, dissolved in ACN, was repeatedly injected. For example, the *N*-Cl-BA and BA peak areas were not consistent without formic acid (Fig. S10a) but were consistent after adding formic acid (Fig. S10b). These results indicated that *N*-Cl-BA likely incurred some type of reaction during the separation process at neutral pH conditions (Fig. S10a) while the lower pH condition minimized this effect (Fig. S10b).

Several strategies were then tested to see how samples from the kinetic experiments could be quenched. The first option was to run samples directly onto the LC system where no specific quenching agent was added but the reaction was quenched or terminated by simply separating the compounds by way of the column. This option was not possible though because it required chlorine to be injected as well, and under the lowered pH condition of the eluent with formic acid, BA loss appeared to be accelerated by a reaction occurring after injection (Fig. S11). The data provided in Fig. S11 demonstrated this effect well. In this figure, the responses of the unquenched samples with formic acid were lower over time than the samples extracted by

liquid/liquid extraction and analyzed by the GC/MS, a method later demonstrated to provide accurate BA loss values (see later discussions for more details). Alternatively, the responses of BA initially decreased slightly but then increased again when running unquenched samples without formic acid (Fig. S11). This effect was likely due to the instability of *N*-Cl-BA under neutral pH conditions, as described before, where *N*-Cl-BA potentially hydrolyzed back to form BA (Fig. S11). These results subsequently indicated that a quenching agent must be added to the samples to fully remove the residual chlorine prior to HPLC injection.

Following this, the effect of various quenching agents including SO_3^{2-} , ascorbic acid and phenol, were all tested and found to convert *N*-Cl-BA back to BA to varying degrees. The use of NH_4Cl as a “soft” quenching agent was also considered here since it was previously known to prevent the reversal of several *N*-Cl containing compounds.⁸ However, this approach was inappropriate for these experiments because it involved increasing the pH to ~8.3 to initially form NH_2Cl . This pH increase could potentially enhance the hydrolysis of *N*-Cl-BA to reform BA (Scheme 1a in main text), which was an artefact that was not desired. Therefore, the role of SO_3^{2-} , ascorbic acid and phenol was instead evaluated by injecting a 15-20 mg/L standard of the *N*-Cl mix onto the HPLC. Prior to the injection, the sample was either exposed or not exposed to a particular quenching agent. The responses from either condition were then compared to each other in terms of their resulting *N*-Cl-BA and BA peak areas (Figs. S12 and S13). First, SO_3^{2-} and ascorbic acid ($[\text{ascorbic acid or } \text{SO}_3^{2-}]_0 = 0.4 \text{ mM}$; $[\text{ascorbic acid}]_0/[\text{N-Cl-BA}]_0 \approx 9.3$) were found to immediately ($< 30 \text{ s}$) convert *N*-Cl-BA back to BA (Fig. S12). Therefore, SO_3^{2-} as a quenching agent was used later to indirectly measure the *N*-Cl-BA concentration by subtracting the BA concentration (determined using a successful quenching approach via the GC/MS; see next section) from the LC-derived BA concentration when adding SO_3^{2-} ($= [\text{BA}] + [\text{N-Cl-BA}]$).

In addition, phenol was tested as a quenching agent. In this procedure, phenol was added in considerable excess to free chlorine ($[\text{phenol}]_0/[\text{HOCl}]_0 = 50$) in order for the reaction between phenol and free chlorine ($k_{\text{app}} = 28 \text{ M}^{-1}\text{s}^{-1}$ at pH 7, 25 °C⁹) to out-compete the reaction of BA with free chlorine ($k_{\text{app}} \sim 10^{-3}\text{-}10^{-1} \text{ M}^{-1}\text{s}^{-1}$ for amides at pH 7.2-7.4¹⁰). However, this approach was also found to be unsuccessful since phenol also converted the *N*-Cl-BA back to BA over time. This result was clearly observed in Fig. S13 when phenol was initially added to a sample of the *N*-Cl mix, representing $t = 0$ min, and then was injected repeatedly onto the HPLC after different reaction times. In this case, the BA concentration, calculated based on its known calibration curve, steadily increased while the *N*-Cl-BA peak area steadily decreased for up to 50 min (Fig. S13). Alternatively, the responses from the control experiment, where the *N*-Cl mix (15 mg/L) was dissolved into the buffer at pH = 7.0 alone, were more stable over 50 min in which the BA and *N*-Cl-BA peak area only increased or decreased slightly (Fig. S13). These slight changes in responses of the control experiment were probably due the fact that the sample was residing in water at a pH of 7.0 and likely experienced a small amount of hydrolysis to form BA over 50 min (Scheme 1a in main text). Subsequently, these data indicated that phenol could also convert the *N*-Cl-BA back to BA, and thus was not appropriate to serve as a quenching agent for samples containing the *N*-Cl-BA compound.

Thus, due to these results, the LC-based methods incurred several limitations in this study for assessing the compounds of interest. First, these methods required that the solutions to be quenched prior to injection onto the LC system. However, since all of the quenching agents that were tested including SO_3^{2-} , ascorbic acid or phenol also reacted with the *N*-Cl moiety, none of these agents could be used to assess the loss of BA when *N*-Cl-BA served as the dominant by-product.

Approach 2: Sample Quenching Coupled with GC/MS analysis.

In this approach, the use of liquid-liquid extraction was deemed successful in terminating all of the chlorinating reactions because of two effects. First, certain charged chlorinating agents, such as OCl^- , were considered to remain in the aqueous phase and not be transferred.¹¹ Second, certain chlorinating agents that are more non-polar (e.g. Cl_2) could plausibly be extracted but were experimentally determined to not undergo any further chemical reactions within the organic solvent phase. This was determined through control experiments where the extracted organic solvent phase was immediately (< 10 min) injected onto the GC/MS but where the same sample was then repeatedly injected over 24 h. The BA concentration was stable over this time frame.

Thus, the extraction procedure consisted of the following steps. First, samples (9 mL) at each time point were taken and extracted for 1 min with 1.5 mL DCM which led the sample to be concentrated by a factor of 6. The DCM solvent also contained 3.0 mg/L naphthalene-d8, which served as an internal standard. The recovery of BA during the extraction was calculated by comparing two different calibration curves, which were obtained by either (i) dissolving 2.5-15 μM BA into the aqueous phase and extracting it by DCM, and (ii) directly dissolving 15-90 μM BA (accounting for the 6-fold concentration factor) into DCM. The obtained calibration curves were similar (Fig. S14). The recovery of all other model compounds by this same extraction technique were considered to be similar given that their chemical structures were similar to that of BA. In addition, the extraction time of 1 min was considered to be minimal when compared to the overall time frame of the reactions tested, which fell over 0.3 to 48 h. A small volume (1 mL) of the DCM layer was then transferred to an autosampler vial and injected onto the GC/MS.

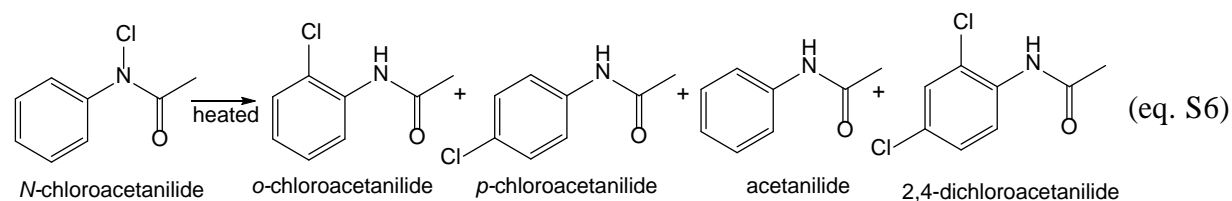
The compounds were then analyzed by GC/MS (Finnigan PolarisQ) using liquid injection. Samples (1 μL) were injected at 180 °C using a 1:10 split ratio onto a HP-5MS (30 m \times 0.25 mm

× 0.25 μm) column. The oven program was held at 80 °C for 1 min, ramped to 240 °C at 25 °C/min, and then held at 240 °C for 4 min. The MS analysis was conducted using electron ionization (70 eV) in positive mode. The MS was run in selected ion monitoring (SIM) mode, and the parameters for each analyte including molecular weight (MS), base peaks (m/z) and ions used for quantifications were summarized in Table S4. The MDLs for BA, *p*-Cl-BA, *o*-Cl-BA, *m*-Cl-BA, 2,4,6-(CH₃)₃-BA, and 2,4,6-Cl₃-BA were 42, 97, 17, 95, 60 and 360 nM, respectively.

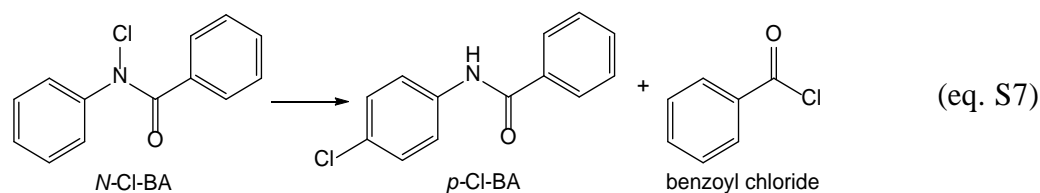
Additional testing was also conducted in order to validate that the liquid-liquid extraction technique quenched the samples in an accurate manner. An experiment was conducted to expose BA to HOCl in the presence of Cl⁻ at pH 4.0 (Fig. S15), where < 10 % of *N*-Cl-BA formed (see details in the Results and Discussion section of the main text). This fact enabled samples from these experiments to be quenched using two different techniques, liquid-liquid extraction and analysis via GC/MS, and SO₃²⁻ quenching and analysis via HPLC, which could then be cross-compared with each other. For this experiment, the data were either plotted as a function of BA concentration (Fig. S15a) or as a pseudo-first order loss (Fig. S15b). The results indicated that both quenching techniques exhibited close to identical kinetic trends where their observed rate constants (*k*_{obs}) were similar (2.5×10⁻³ and 2.9×10⁻³ s⁻¹) (Fig. S15b). In the end, these results confirmed that liquid-liquid extraction was a valid quenching technique and could be further used to measure the kinetic loss of the model compounds evaluated in this study.

Moreover, one last concern for this approach was related to the fact that the *N*-Cl compound (e.g. *N*-Cl-BA) could potentially decompose to reform the parent compound (e.g. BA) and other by-products within the injection port, given its high temperature of 180 °C. This concern arose because of previous literature, which indicated that *N*-Cl compounds were not thermally stable and could undergo decomposition when heated.^{12, 13} For example, *N*-chloroacetanilide was

observed to decompose to *o*- (conversion of 17-18%) and *p*- (41-51%) chloroacetanilide, acetanilide (6.3%) and 2,4-dichloroacetanilide (4.0-7.0%) at 100°C (eq. S6).¹³



Also, *N*-Cl-BA was observed to decompose to *p*-Cl-BA and benzoyl chloride at 120-130 °C (eq. S7).¹²



Initially, it was clear that the *N*-Cl compound (e.g. *N*-Cl-BA) did not form *o*- and *p*-Cl BA since certain experiments (e.g. high pH experiments; see results and discussion section in the main text) only formed *N*-Cl-BA while *o*- and *p*-Cl-BA formation was not observed. Alternatively, another concern was regarding whether the *N*-Cl compound (e.g. *N*-Cl-BA) could decompose to the parent compound (e.g. BA). This effect would alter the true kinetic loss of BA over time that was measured by this instrument. Therefore, to evaluate if this was the case, the injection port temperature was varied from 160 to 260 °C to assess how the peak area of BA was subsequently affected. This procedure was used since it was hypothesized that if *N*-Cl-BA did decompose to BA in the injection port, the extent of decomposition (e.g. [decomposed *N*-Cl-BA]/[injected *N*-Cl-BA]) would increase as the injection port temperature increased. In addition, various concentrations of *N*-Cl-BA concentrations were injected, since it was also suspected that the higher concentration of *N*-Cl-BA might have larger effect.

In order to test this, two types of samples were evaluated including pure BA standards (5.0 and 10 μM), and samples taken at certain time points (3 to 29 h) during the reaction of BA with free chlorine at pH 7 and 9. These latter samples were determined to contain both BA, which were directly measured based on a calibration curve, and ~ 0.5 to $2.8 \mu\text{M}$ *N*-Cl-BA, which was indirectly quantified using the sulfite (SO_3^{2-}) quenching approach. The BA standards were run so that they could serve as control experiments to account for any response differences driven solely by changing the injection port temperature. The results indicated that as the injection port temperature increased, the peak areas of BA from both pure BA standard and the samples containing both BA and *N*-Cl-BA decreased slightly (Fig. S16).

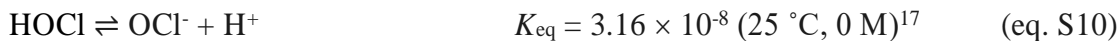
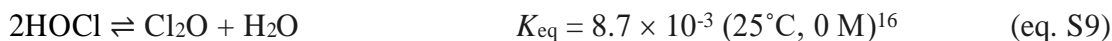
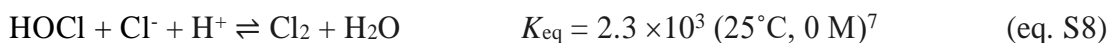
In the end, such results suggested that either: (i) the decomposition of *N*-Cl-BA to BA was not significant over this temperature range, or (ii) the *N*-Cl-BA present in solution had already fully converted to BA at the starting injection port temperature of 160°C , such that any further increase in temperature was not needed to initiate greater decomposition. However, additional evidence from previous literature supports the fact that option (i) rather than option (ii) occurred. As mentioned above, only 6.3% of *N*-Cl-acetanilide decomposed back to its parent compound, acetanilide, when heated.¹³ Moreover, another study suggested that the thermal decomposition of *N*-Cl compounds (e.g. *N*-chloroacetanilide) to form the amide was highly solvent dependent.¹⁴ Their results found that the chlorine could be transferred from the *N*-Cl compound to form anilide in solvents (e.g. acetoacetic ester) that readily underwent substitution.¹⁴ Since the samples were extracted by DCM where substitution reactions with chlorine required much higher temperatures ($400\text{--}650^\circ\text{C}$),¹⁵ it further supported the fact that *N*-Cl-BA did not decompose to a significant extent to form BA during GC/MS analysis.

Text S6. Measurement of chloride (Cl⁻) using the IC.

The Cl⁻ concentration in various buffers and the free chlorine stock was measured by the IC (Metrohm 940 Professional IC Vario), as done previously⁷. Separation occurred using an A Supp 7-250/4.0 column at 30 °C. The eluent contained 1.0 mM Na₂CO₃ and 4.0 mM NaHCO₃ and was run at a flow rate of 0.7 mL/min. The MDL for Cl⁻ was 1.2 µM.

Text S7. Calculations of equilibrium concentrations for the various chlorinating agents.

The equilibrium concentrations for HOCl, OCl⁻, Cl₂ and Cl₂O were calculated by simultaneously solving eqs. S8, S9 and S10 with their known equilibrium constants and initial concentrations of HOCl and Cl⁻ using Solver in Excel.



Each equilibrium constant was adjusted for ionic strength according to each experimental condition using the Davies equation.¹⁸ The equilibrium concentration of each chlorinating agent under each tested condition are summarized in Table S5.

Text S8. Determination of second-order rate constants

Species-specific rate constants including k_{Cl_2} , $k_{\text{Cl}_2\text{O}}$, and k_{HOCl} were obtained by fitting the experimentally determined values of k_{obs} and concentrations of HOCl, OCl⁻, Cl₂ and Cl₂O for experiments conducted at pH 4.0 to eq. S11.

$$k_{\text{obs}} = k_{\text{HOCl}}[\text{HOCl}] + k_{\text{Cl}_2\text{O}}[\text{Cl}_2\text{O}] + k_{\text{Cl}_2}[\text{Cl}_2] + k_{\text{OCl}^-}[\text{OCl}^-] \quad (\text{eq. S11})$$

First, the equilibrium concentrations for HOCl, OCl⁻, Cl₂ and Cl₂O were obtained (see details in Text S7). Second, the values of measured k_{obs} and calculated equilibrium concentrations were fitted through a least-squares regression into eq. S11 to achieve the species-specific rate constants of k_{HOCl} , k_{OCl^-} , k_{Cl_2} and $k_{\text{Cl}_2\text{O}}$ which were obtained sequentially. This least-squares regression was performed in OriginPro 2016. For this study, the approach consisted of the following steps. Initially, the model only applied data where Cl⁻ was amended to the solutions. This limitation was incurred so that the contribution of $k_{\text{Cl}_2}[\text{Cl}_2]$ to the reaction could be considered to be much greater than the sum of the $k_{\text{OCl}^-}[\text{OCl}^-]$, $k_{\text{Cl}_2\text{O}}[\text{Cl}_2\text{O}]$ and $k_{\text{HOCl}}[\text{HOCl}]$ contributions due to the known higher reactivity of Cl₂. The resulting value of $k_{\text{Cl}_2} = (7.6 \pm 0.19) \times 10^1 \text{ M}^{-1}\text{s}^{-1}$ was obtained, and the contribution of HOCl, OCl⁻, and Cl₂O ($k_{\text{Cl}_2\text{O}}[\text{Cl}_2\text{O}] + k_{\text{HOCl}}[\text{HOCl}] + k_{\text{OCl}^-}[\text{OCl}^-]$) were later determined to be <10% of k_{obs} which validated that the original assumption that was made was indeed correct. After this, all the other data except for the Cl⁻ amended experiments were used to solve for k_{HOCl} , k_{OCl^-} and $k_{\text{Cl}_2\text{O}}$ using the fixed k_{Cl_2} value ($= 7.6 \times 10^1 \text{ M}^{-1}\text{s}^{-1}$), and k_{HOCl} and k_{OCl^-} were determined to be $(2.1 \pm 0.22) \times 10^{-2}$ and $(1.7 \pm 1.5) \times 10^1 \text{ M}^{-1}\text{s}^{-1}$, respectively. However, a large uncertainty was observed when simulating the data for $k_{\text{Cl}_2\text{O}}$, which was determined to be $(0.021 \pm 1.9) \times 10^3 \text{ M}^{-1}\text{s}^{-1}$.

484 **References:**

- 485 1. Thomm, E. W. C. W.; Wayman, M., N-Chlorination of secondary amides. II. Effects of
486 substituents on rates of N-chlorination. *Can. J. Chem.* **1969**, 47, (18), 3289-3297.
- 487 2. Voutchkov, N., *Pretreatment for reverse osmosis desalination*. Amsterdam, Netherlands :
488 Elsevier: 2017.
- 489 3. Holland, H. D., *The chemistry of the atmosphere and oceans*. New York : Wiley: New
490 York, 1978.
- 491 4. Cotruvo, J. A., *Desalination Guidelines Development for Drinking Water: Background*.
492 In World Health Organization: Washington D.C., 2005.
- 493 5. Naumov, P.; Topcu, Y.; Eckert-Maksić, M.; Glasovac, Z.; Pavošević, F.; Kochunnonny,
494 M.; Hara, H., Photoinduced rearrangement of aromatic N-chloroamides to chloroaromatic
495 amides in the solid state: inverted $\Pi(N)$ - $\Sigma(N)$ occupational stability of amidyl radicals. *J. Phys.*
496 *Chem. A* **2011**, 115, (26), 7834.
- 497 6. Chen, T., Spectrophotometric determination of microquantities of chlorate chlorite
498 hypochlorite and chloride in perchlorate. *Anal. Chem.* **1967**, 39, (7), 804-&.
- 499 7. Sivey, J. D.; McCullough, C. E.; Roberts, A. L., Chlorine Monoxide (Cl₂O) and
500 Molecular Chlorine (Cl₂) as Active Chlorinating Agents in Reaction of Dimethenamid with
501 Aqueous Free Chlorine. *Environ. Sci. Technol.* **2010**, 44, (9), 3357-3362.
- 502 8. Dodd, M.; Huang, C., Transformation of the antibacterial agent sulfamethoxazole in
503 reactions with chlorine: Kinetics mechanisms, and pathways. *Environ. Sci. Technol.* **2004**, 38,
504 (21), 5607-5615.
- 505 9. Gallard, H.; Von Gunten, U., Chlorination of phenols: Kinetics and formation of
506 chloroform. *Environ. Sci. Technol.* **2002**, 36, (5), 884-890.

- 507 10. Pattison, D.; Davies, M., Kinetic analysis of the reactions of hypobromous acid with
508 protein components: Implications for cellular damage and use of 3-bromotyrosine as a marker of
509 oxidative stress. *Biochemistry-US* **2004**, *43*, (16), 4799-4809.
- 510 11. Harris, D. C., *Quantitative Chemical Analysis*. 8 ed.; W. H. Freeman and Company: New
511 York, NY, 2010.
- 512 12. Chattaway, F. D.; Orton, K. J. P., CIV.—A series of substituted nitrogen chlorides and
513 their relation to the substitution of halogen in anilides and anilines. *J. Chem. Soc., Trans.* **1899**,
514 *75*, (0), 1046-1054.
- 515 13. Bradfield, A. E., LI.—The chlorination of anilides. Part II. The decomposition of N -
516 chloroacetanilide by heat. *J. Chem. Soc.* **1928**, *0*, (0), 351-352.
- 517 14. Beard, C. C.; Boocock, J. R. B.; Hickinbottom, W. J., 107. Molecular rearrangements.
518 Part IV. The thermal rearrangement of N-chloroacetanilide. *J. Chem. Soc.* **1960**, 520-522.
- 519 15. Carlisle, P. J. Chlorination of Methyl Chloride. 1933.
- 520 16. Voudrias, E.; Redden, G.; Reinhard, M., Hydrolysis Constants of Chlorine Monoxide and
521 Bromine Chloride in Water. *Water Chlorination: Chemistry, Environmental Impact and Health*
522 *Effects*. Proceedings of the Sixth Conference on Water Chlorination: Environmental Impact and
523 Health Effects, Oak Ridge , Tennessee, May 3-8, 1987. Lewis Publishers, Inc., Chelsea,
524 Michigan. National Science Foundation Grant CEE-81-17561, 1989, 6, 859-870.
- 525 17. Morris, J. C., The Acid Ionization Constant of HOCl from 5 to 35°. *J. Phys. Chem.-US*
526 **1966**, *70*, 3798-3805.
- 527 18. Langmuir, D., *Aqueous environmental geochemistry*. Upper Saddle River, N.J. : Prentice
528 Hall: Upper Saddle River, N.J., 1997.
- 529